Kinetic Monte Carlo simulations of the interaction of oxygen with Pt(111)

Christian Sendner[1] and Axel Groß[2]

[1] *Physik-Department T30, Technische Universität München, D-85747 Garching, Germany*
[2] *Institut für Theoretische Chemie, Universität Ulm, D-89069 Ulm, Germany*

(Dated: February 1, 2007)

The adsorption, dissociation, diffusion, and desorption of oxygen interacting with the Pt(111) surface has been studied using kinetic Monte Carlo simulations. This study has been motivated by uncertainties in the theoretical and the experimental derivation of O_2/Pt(111) reaction barriers. The simulations reproduce all known experimental data within basically one set of parameters, thus yielding microscopic insights into the elementary reaction steps occuring in the interaction of oxygen with Pt(111) and providing reliable estimates for adsorption energies and diffusion and desorption barriers. In particular, we confirm that the distance of oxygen atoms directly after dissociation is caused by ballistic *hot atom* motion rather than by diffusive motion. We address the equilbrium structure of oxygen atoms at high coverages. At low temperatures, chains of oxygen pairs are formed. We show that this mechanism can be explained by a lowered dissociation in the vicinity of already adsorbed atoms. Finally we discuss the role of the lateral interaction between the oxygen atoms in the oxygen desorption process.

PACS numbers: 68.43.Bc, 68.43.Mn, 82.65.+r

I. INTRODUCTION

The interaction of oxygen with Pt(111) represents one of the model systems in surface science, the interest in this system also being fueled by the fact that the adsorption of O_2 on Pt is a crucial microscopic reaction step occurring in the car-exhaust catalyst. The adsorption of O_2/Pt(111) has been studied in detail experimentally [1–7]. The adsorption dynamics is quite complex since O_2 can adsorb both molecularly as well as dissociatively on Pt(111) [8–15]. In spite of these numerous studies on this seemingly simple system, there are still several aspects of the O_2 dissociation dynamics and kinetics on Pt(111) that remain unclear. For example, only recently it has been shown by *ab initio* based molecular dynamics simulations that in this system the whole adsorption probability as a function of the kinetic energy can be understood in terms of trapping into chemisorbed molecular precursor states without invoking any physisorption or dissociative adsorption [16–18]. The experimental observation [3, 6, 7] that O_2 does not dissociate on cold Pt(111) surfaces even at kinetic energies that are much greater than the dissociation barrier could be explained by simple steric arguments based on the specific shape of the potential energy surface [16].

Summarizing the known experimental facts, it is well-known that at very low temperatures (T<30 K) molecular oxygen is physisorbed on Pt(111) with a binding energy of about 0.1 eV [10, 13]. With increasing temperature, the physisorbed oxygen is converted to a chemisorbed molecular state or it desorbs with a desorption peak at 45 K in temperature-programmed desorption (TPD) spectra [13]. There are two distinct chemisorbed states for molecular oxygen, the non-magnetic peroxo (O_2^{2-}) and the paramagnetic superoxo (O_2^-) state [12, 19, 20] which can be spontaneously accessed from the gas phase [19–21]. For surface temperatures above 140-160 K, these chemisorbed molecules either desorb [13] or dissociate on the surface [14]. The created oxygen atoms occupy two fcc sites on the Pt(111) surface separated by a mean difference of two Pt lattice constants [14]. With further heating of the surface, the atoms are able to diffuse on the surface. The diffusion barrier was experimentally determined to be 0.43 eV with a pre-exponential factor of $4 \cdot 10^9$ s^{-1} [14]. The occupation of the hcp sites with oxygen atoms is metastable only for temperatures smaller than 50 K [5]. The adsorption of molecular oxygen at intermediate temperatures leads to a p(2x2) structure of atomic oxygen on the surface [22] which corresponds to a saturation coverage of 0.25 monolayers. Higher concentrations above 0.25 monolayers of atomic oxygen can be realized by exposing either NO_2 [23] or ozone (O_3) [24] to the Pt surface.

As far as the first-principles description of O_2/Pt(111) is concerned, in particular within the framework of density functional theory (DFT), it suffers from the fact that the molecular properties of O_2 are poorly reproduced using state-of-the-art exchange-correlation functionals within the generalized gradient approximation (GGA) [25]. For example, the binding energy of the O_2 dimer is overestimated by more than 0.5 eV using the popular PW91 functional [26]. The binding energies of the O_2 molecular chemisorption state are in the range of 0.6 - 0.8 eV according to PW91-DFT calculations [20, 27]. The RPBE functional [25] gives a better description of the O_2 molecular properties, however, it predicts the binding energy of the molecular chemisorption states to be 0.1 eV [28] which seems to be too low. Comparing the results obtained using the PW91 and the RPBE functional confirms that there is an intrinsic uncertainty in the GGA calculations of about 0.5 eV. As far as the diffusion of oxygen atoms on Pt(111) is concerned, DFT calculations yield a diffusion barrier of 0.58 eV with a prefactor of $2.6 \cdot 10^{12}$ s^{-1} [29]. These numbers might

in fact be more reliable because differences between similar configurations are considered where error cancellation effects are operative.

The situation regarding the uncertainty in the values derived by first-principles calculations is doubtless not very satisfactory. Experimentally, however, adsorption energies and diffusion barriers are never directly measured but only indirectly via their consequences on the desorption and diffusion flux. Thus there is also an uncertainty about the experimentally derived values since often assumptions such as the kinetic order of the process enter the derivation of the barriers.

We have therefore addressed the adsorption, dissociation, diffusion and desorption of oxygen interacting with Pt(111) using kinetic Monte Carlo (kMC) simulations. The parameters entering the kMC formalism have been motivated by the DFT results, but adjusted in order to match the experimental results. Dynamical Monte Carlo simulations of O_2 adsorption and dissociation on Pt(111) were already performed before [30], however, these simulations were restricted to low surface temperatures below 200 K whereas we have considered surface temperatures up to 1000 K. In addition, we have addressed further aspects of the O_2-Pt interaction such as the structure formation at low surface temperatures. We have been able to reproduce the known experimental results with basically one set of parameters thus providing comprehensive microscopic insights into the interaction of oxygen with Pt(111).

II. COMPUTATIONAL DETAILS

Kinetic Monte Carlo simulations can be regarded as a coarse-grained, lattice-based atomistic simulation technique [31–34]. In a kMC-simulation, every possible process of a system is described by a rate constant R_i which is the probability for a particular event per unit time. It can for example be calculated using *transition state theory* [35]. In the harmonic approximation, the rate constants show an Arrhenius behavior as a function of temperature,

$$R_i = \nu_0 \exp\left(-\frac{E_a}{k_B T}\right) , \qquad (1)$$

where E_a denotes the energy barrier for a particular process and ν_0 is the so-called attempt frequency. The first step in any kMC simulation is to set up a list of all possible processes. Then a single process is chosen randomly with a probability according to its rate R_i by drawing a random number ρ and selecting the process j that fulfills

$$\sum_{i=1}^{j-1} R_i \leq \rho R < \sum_{i=1}^{j} R_i \qquad (0 \leq \rho < 1) , \qquad (2)$$

where R denotes the overall rate ($R = \sum_{i=1}^{N} R_i$) of all N possible processes of the system and ρ is a random number between zero and one. After each kMC step, the time is advanced according to

$$\Delta t = -\ln(\rho_2)/R \qquad 0 < \rho_2 \leq 1 , \qquad (3)$$

where ρ_2 is a second random number. Then a new event table is set up, and the procedure starts again.

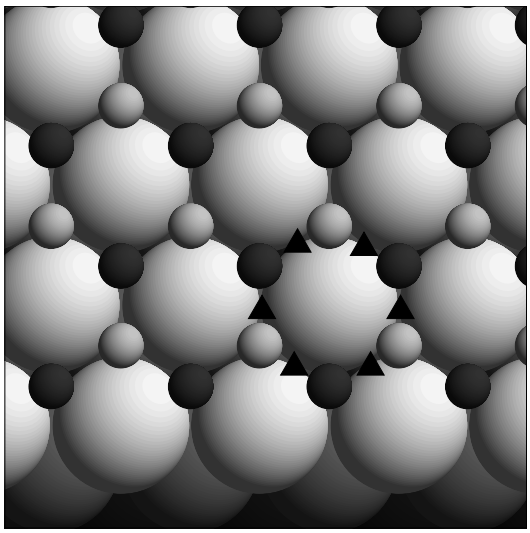

FIG. 1: Illustration of the Pt(111) surface and the grid points used in the kMC simulations. The small dark circles label the fcc sites, the light small circles the hcp sites. The black triangles mark the bridge positions.

For the underlying lattice describing the Pt(111) substrate, a hexagonal lattice with one fcc, one hcp site and three bridge sites per unit cell was used (see Fig. 1). The atoms are assumed to be only located at the fcc sites since the hcp sites are energetically unfavorable by 0.45 eV [29], whereas the molecules are able to occupy the fcc and hcp hollow and the bridge sites. For the simulations at lower temperature, periodic boundary conditions were applied with a grid of 200×200 sites per unit cell. A smaller grid of 60×60 sites was employed for the high temperature simulations due to the much larger computational effort when the rate constants are significantly increased.

In order to simulate the heating of the surfaces, which is especially important for the determination of the TPD spectra, the following scheme was used. The temperature was kept fixed during 0.5 seconds and the temperature dependent values were calculated as a time average. After simulating the system over this time, the temperature was increased according to the applied heating rate, the variables for the new temperature were computed and the system was simulated for the next 0.5 seconds.

One important aspect of processes on surfaces is the lateral interaction of adsorbates which changes the adsorption energy as a function of the coverage. Thereby, it also affects the barriers for diffusion and desorption. In this work, we have modeled the influence of the oxygen

coverage by

$$E_a = E_a^0 - \sum_{i=1}^{3} \epsilon_i \sqrt{n_i} \ , \qquad (4)$$

where n_1, n_2 and n_3 are the number of next-nearest, second-nearest and third-nearest neighbor oxygen atoms, respectively. The square-root dependence in the number of nearest neighbor represents an assumption, but is motivated by the fact that the strength of chemical bonds in the tight-binding approximation also shows a square root dependence on the number of binding partners [36].

III. RESULTS

A. Dissociation

Oxygen can exist both in molecular and in atomic adsorption states on Pt(111). On cold platinum surfaces below 160 K, O_2 does not dissociate, even if the molecules are impinging on the surface with kinetic energies of more than 1 eV [3, 6, 7]. Using *ab initio*-based tight-binding molecular dynamics simulations [16] it was recently shown that this is due to steric hindrance making the direct access of the dissociation channel rather unlikely. The O_2 dissociation on Pt(111) is therefore a two-step process: First the molecule becomes trapped molecularly, and only in a second step it dissociates at sufficiently high surface temperatures in an activated process which can be described by a rate constant of the form of eq. (1). The height of the dissociation barrier has been estimated to be about 0.3 eV according to TPD experiments [8]. The analysis of molecular beam experiments at different surface temperatures yielded a ratio between the prefactor for oxygen desorption (ν_1) and for dissociation (ν_2) of 0.12 [2], leading to a value for ν_2 of $1.2 \cdot 10^{12} s^{-1}$ when inserting a generic prefactor for the molecular desorption of $10^{13} s^{-1}$.

In experiments using scanning tunneling microscopy (STM) the distribution of interatomic O-O distances after the O_2 dissociation on Pt(111) at 160 K and 163 K was mapped out [14]. The measured distribution was strongly peaked at two Pt lattice constants, i.e., at twice the Pt-Pt nearest-neighbor distance. These results were interpreted as being due to a *hot* atoms that travel ballistically directly after the dissociation, as had also initially been suggested to explain results for the distribution of oxygen atoms on Al(111) after dissociative adsorption [37]. On the other hand, two lattice units are also the equilibrium distance of an oxygen overlayer on Pt(111) created by the dissociation of O_2. In order to find out whether the distribution of O atoms after dissociation is due to ballistic or to thermal motion, we have performed kMC simulations in which we have assumed that dissociated oxygen atoms are initially only separated by one lattice unit and then diffuse thermally by single jumps.

The simulations were started with two oxygen atoms on adjacent fcc sites. Then, the atoms were allowed to diffuse for a certain time period Δt, which was varied between 1 s and 1 h since the time used in the experiment [14] to measure the distance distribution was not known. After this simulation time, the distance of the two atoms is determined. In order to get good statistics, the simulations were carried out for 10^6 oxygen pairs. We assumed the diffusion barrier to be dependent on the position of the second atom, however, the prefactor was assumed to be constant at $\nu_0 = 2.6 \cdot 10^{12}\ \mathrm{s}^{-1}$. The heights of the barriers were adjusted in order to reproduce the experimental distribution.

In table I, the energy barriers necessary to get the experimental distance distribution are shown. The error in the occupation numbers was below 1%. The diffusion events are labeled $d_i \to d_f$, where d_i and d_f are the distances of the diffusing oxygen atom from the other oxygen atom before and after the diffusion event, respectively. It turned out, that the processes $1 \to 1$, $\sqrt{3} \to 1$ and $2 \to 1$ are not necessary to reproduce the distribution of the intrapair distances. Because of the strong repulsive interactions between adjacent oxygen atoms [38] these procesesses are very rare and can be neglected.

Experimentally, it is well-known that oxygen atoms form a $p(2 \times 2)$ structure on Pt(111) [39]. As we will show in the next section, this requires that there is a strong repulsive interaction between next-nearest neighbors ($d = 1$), a weak repulsive interaction between second-nearest neighbors ($d = \sqrt{3}$) and an attractive interaction between third-nearest neighbours ($d = 2$). Hence, the energy barriers for diffusion jumps for an atom with $d_i = 1$ should be significantly lower than for the other jumps, but this is not the case. Hence the diffusion barriers needed to reproduce the O-O distances after dissociation would not reproduce the right equilibrium structure of oxygen atoms. This is an indication that indeed these distances are due to ballistic and not diffusive processes.

Furthermore, in the STM experiment [14] the O-O distances after dissociation were also determined for a slightly higher surface temperature of 163 K. The kMC

	Simulation time (s)			
jump $d_i \to d_f$	1	12.5	100	3600
$1 \to \sqrt{3}$	0.4110	0.4425	0.4715	0.5189
$1 \to 2$	0.3987	0.4370	0.4652	0.5176
$\sqrt{3} \to 2$	0.4200	0.4476	0.4789	0.5236
$\sqrt{3} \to \sqrt{7}$	0.4235	0.4595	0.4861	0.5374
$2 \to \sqrt{3}$	0.4523	0.4859	0.5264	0.5680
$2 \to \sqrt{7}$	0.4485	0.4835	0.5240	0.5654
$2 \to 3$	0.4459	0.4799	0.5088	0.5572

TABLE I: Diffusion barriers in eV, necessary to reproduce the experimental distribution of O-O distances at 160 K [14] for different kMC simulation times. d_i and d_f are the distances of the diffusing oxygen atom from the other oxygen atom before and after the diffusion event, respectively.

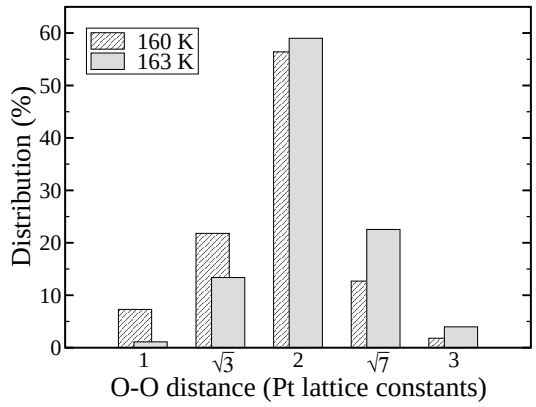

FIG. 2: Calculated distribution of the O-O interpair distances at 160 K and 163 K using the energy barriers listed in Table I for a simulation time of 1 s.

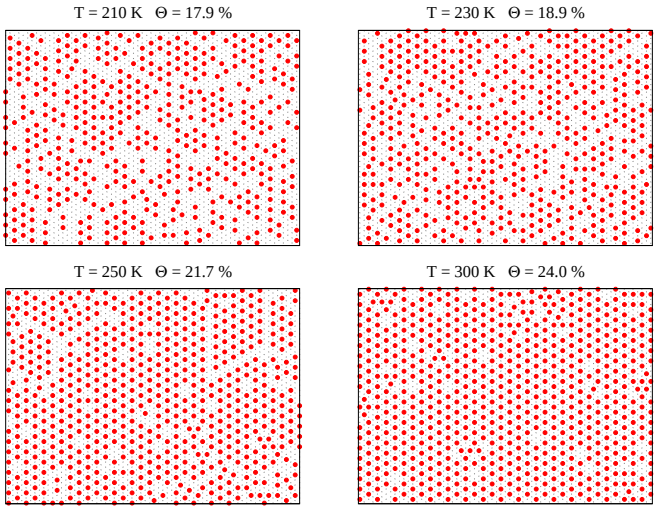

FIG. 3: Snapshots of the Pt(111) surface for a O_2 pressure of 10^{-2} Pa. The dark circles are the oxygen atoms. The surface was heated from 200 K to 300 K with a heating rate of 2 K/s. The pictures show a 100 x 72 fraction of the used 200 x 200 grid at 210 K, 230 K, 250 K and 300 K.

results for the two different temperatures are compared in Fig. 2. The results are as expected: for higher temperature the mean distance between the two atoms is shifted to a larger value. However, in the experiment more pairs with distances $d = 1$ and $d = \sqrt{3}$ have been found at the higher temperature which is in qualitative disagreement with the kMC simulations. This is another indication that the experimental distance distribution after dissociation is not caused by thermally activated single jumps but rather by a ballistic hot atom motion.

Hence we have assumed in the following that the O atoms after dissociations are located at two fcc sites that are two Pt lattice constants apart from each other. Thus, the molecules are only allowed to dissociate if there are two fcc sites in a distance of two lattice constants available. Because of the strong repulsive interaction between oxygen next-nearest neighbours, the dissociation is furthermore suppressed if the two fcc sites have oxygen next-nearest and second-nearest neighbors.

B. Saturation Coverage of Oxygen on Pt(111) upon O_2 exposure

Experimentally, it is well-established that oxygen atoms that have been dosed as O_2 molecules to the Pt(111) surface form a p(2x2) structure on the surface corresponding to a saturation coverage of 0.25 monolayer (ML) [39]. The model of the dissociation process of O_2 on Pt(111) just described in the previous section has been used to address the saturation coverage of oxygen on Pt(111) when O_2 is dosed to the surface. For the height of the O_2/Pt(111) dissociation and the desorption barrier, we used experimentally derived values of 0.3 eV [8] and 0.36 eV [40], respectively. For the barrier for *atomic* diffusion on the clean surface, $E^0_{\rm diff}$, we took the theoretical value of 0.58 eV [29]. The diffusion barrier for the O_2 molecules was set to 0.20 eV in the following.

The coverage dependence of the atomic diffusion barrier was modeled according to eq. (4). In the equilibrium p(2x2) structure, the oxygen atoms are located at third-nearest neighbor sites. Hence we expect that the lateral interaction is repulsive for next-nearest and second-nearest neighbors ($\epsilon_{1,2} > 0$) while it might be attractive for third-nearest neighbors($\epsilon_3 < 0$), as it was also necessary to describe the phase diagram of oxygen on Pt(111) using a lattice-gas Hamiltonian [38].

The saturation coverage of oxygen atoms has been studied for a constant O_2 pressure of 10^{-2} Pa while heating the surface from 200 K to 300 K with a heating rate of 2 K/s. Snapshots of these simulations on a grid of 200×200 lattice points are shown in Fig. 3. It turned out that the interaction parameters $\epsilon_2 = 0.04$ eV and $\epsilon_3 = -0.025$ eV are best suited to reproduce the experimental findings while no oxygen atoms were allowed to be at adjacent sites.

For temperatures lower than 250 K, atomic diffusion is still frozen in. Therefore islands form which only grow by dissociation events at their edges. Eventually the voids between the oxygen islands become so small, that no further dissociation can occur. The narrow gaps between the islands remain unoccupied and the islands do not coalesce. Because of these gaps, the maximum coverage at 210 K and 230 K is below 20% (see the upper panels of Fig. 3).

For temperature above 250 K, the oxygen atoms begin to diffuse. The islands start to coalesce which opens up uncovered areas where additional molecules are able to adsorb and dissociate. By this mechanism, a coverage of up to 24% can be achieved. At 250 K, there are still grain boundaries between domains of lattice sites that are not in registry. At 300 K, there are only oxygen vacancies in the $p(2 \times 2)$ oxygen overlayer left, in these vacancies, however, no oxygen molecules can adsorb and dissociate.

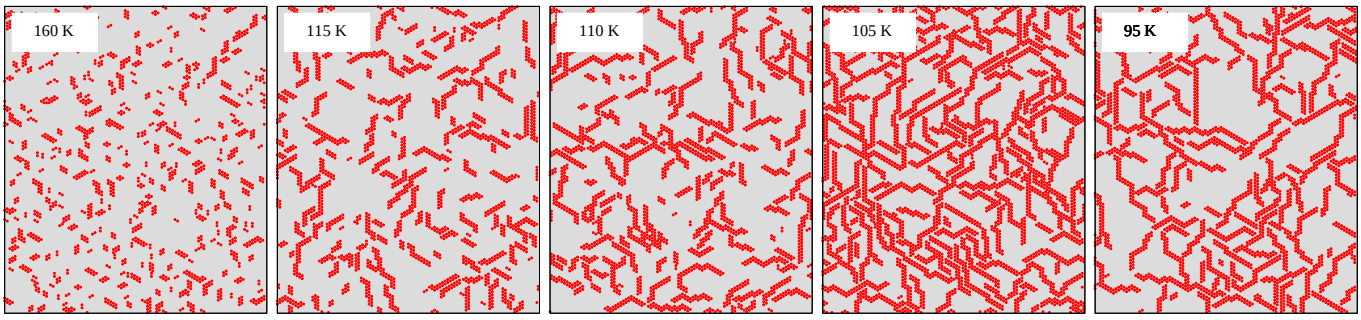

FIG. 4: Structure of oxygen atoms adsorbed on Pt(111) after exposure of O_2 molecules at temperature between 95 and 160 K. The kMC simulations were carried out on a 200×200 grid. The dissociation barrier for the O_2 molecules was lowered from 0.30 eV to 0.25 eV in the vicinity of adsorbed oxygen atoms while the diffusion barrier for the molecules was 0.20 eV.

Therefore the $p(2\times2)$ oxygen layer does not become fully completed.

C. Chains of Adsorbed Oxygen Atoms

Experiments have shown that after the adsorption and dissociation of O_2 on Pt(111) at low temperatures between 100 K and 160 K, the oxygen atoms exhibit a chain-like structure on the surface [41]. Oxygen adsorption at temperatures around 100 K leads to long chains formed by pairs of oxygen atoms that are separated on the average by two Pt lattice units. With increasing temperatures, these chains become shorter, and at 160 K there are mainly pairs of oxygen atoms present on the surface.

It was suggested that this phenomenon could be due to an environment-depending O_2 dissociation barrier [41]. Since the diffusion barrier for O_2 molecules on Pt(111) is rather low, the molecular precursor is relatively mobile. In the vicinity of an atomic oxygen pair, the dissociation barrier for the molecule should be lowered so that the O_2 molecules dissociate preferentially at the end of existing chains. At these temperatures, the atomic diffusion is still frozen in so that the formed chains are stable.

We have tested this hypothesis using the kinetic Monte Carlo algorithm by lowering the dissociation barrier for O_2 molecules in the vicinity of adsorbed oxygen atoms. For the simulations, a 200×200 grid was used. The simulations were stopped after 300 s when 1 Langmuir O_2 was offered at a pressure of 10^{-3} Pa. The resulting oxygen structure for different temperature between 95 and 160 K are shown in Fig. 4. It turned out that a lowering of the dissociation barrier by 0.05 eV from 0.30 eV to 0.25 eV was sufficient to nicely reproduce the experimental results [41]. Because of the increased dissociation probability at the end of existing chains, the oxygen adatoms grow indeed in a quasi-one-dimensional fashion forming long chains.

The resulting structures also depends sensitively on the used diffusion barrier. For an increased diffusion barrier, the chains became shorter. This supports the speculation [41] that the mobility of the molecular precursor is an essential parameter for the structure of the resulting chains. According to our simulations, for a desorption barrier of 0.36 eV from the molecular state, molecular desorption starts at about 130 K. With decreasing temperature, the lifetime of the molecules on the surfaces increases because the desorption rate decreases. And since the diffusion barrier is significantly smaller than the desorption barrier, the mean free path increases with lower temperature because the ratio of the rates for desorption and diffusion decreases. Therefore, the O_2 molecules are able to reach already adsorbed oxygen atoms at low temperatures, thus forming long chains (see the panels for 95 K and 105 K of Fig. 4). At higher temperature, when desorption sets in, the O_2 molecules can no longer propagate over longer distances. Therefore a smaller fraction of molecules reaches the ends of existing O_2 chains so that the chains become shorter (see the panels for 110 K and 115 K of Fig. 4). Finally, at 160 K, there are almost only isolated oxygen pairs present on the surface since adsorbed oxygen molecules rather desorb than diffuse on the surface so that no chains can be formed any more.

D. Associative Desorption

Experimentally it has been observed that oxygen atoms start to desorb associatively at temperatures above 500 K [24]. Because of the strong lateral interaction between the oxygen atoms, the desorption is strongly dependent on the initial coverage. In order to prepare oxygen layers with coverage higher than 0.25 ML, ozone was exposed to Pt(111) so that coverages of up to 0.95 ML were obtained [24]. In subsequent TPD experiments, it was observed that the desorption peak shifted from 810 K to 620 K when the oxygen coverage was increased from 0.03 ML to 0.95 ML.

To describe the associative desorption, we have made the desorption barrier coverage-dependent according to eq. (4). The associative desorption was assumed to occur directly from oxygen atoms that are next-nearest, second-nearest or third-nearest neighbors. If the atom has more than one neighbour at different distances, it

can only associate with the nearest atom per direction. The same interaction energies $\epsilon_i, i = 1-3$ were used both for associative desorption as well as for atomic diffusion, but due to the higher temperatures oxygen atoms located at adjacent sites are now permitted.

The energy barrier for the associative desorption from two oxygen atoms at adjacent fcc sites was calculated using DFT to be 1.83 eV [20]. The coverage in the calculation corresponded to 0.5 ML. Assuming a value of 0.1 eV for ϵ_1, the desorption barrier from the clean surface becomes approximately $E_d^0 \approx 2.0$ eV. This value was used in the following simulations.

The prefactor for the associative desorption was set equal to that for the atomic diffusion ($\nu_0 = 2.6 \cdot 10^{12}$ s^{-1}). We note, however, that the exact value of the prefactor plays a much less important role than the barrier height for the reaction kinetics. Since the rate constants for the atomic diffusion and the associative desorption differ by a factor of up to 10^{10} dependent on the temperature, diffusion events occur much more frequently than desorption events. This makes the determination of desorption spectra very time-consuming. To speed up the computation, the diffusion rate was set to zero after N^2 sequential diffusion steps, where N is the amount of lattice sites in $\hat{x}$ and $\hat{y}$ direction. This is equivalent to the assumption that the distribution of the atoms on the surface corresponds to an equilibrium situation because of the different time scales on which diffusion and desorption events occur. We checked this assumption by increasing the step numbers after which the diffusion was frozen in, and found no difference in the results, which means that the assumption of thermal equilibrium is justified.

In order to simulate the TPD spectra of oxygen desorbing associatively from Pt(111) for different initial coverages between 0.03 and 0.97 ML, a 60×60 grid was used. The heating rate was always 4 K/s. The results were summed over several iterations to obtain better statistics. The starting temperature was chosen low enough so that the atoms can equilibrate on the surface before the associative desorption sets in.

We have varied the lateral interaction parameters ϵ_i in order to obtain good agreement with the experimental TPD spectra [24]. In Fig. 5, we have collected the results of the simulated TPD spectra for small coverages of 0.03 ML and 0.19 ML. The parameter ϵ_3 was varied from -0.01 eV to -0.05 eV while $\epsilon_2 = 0.04$ eV was kept constant. In addition, we used the value $\epsilon_1 = 0.237$ eV which was derived from DFT calculations using a lattice-gas Hamiltonian to describe the phase diagram of oxygen on Pt(111) [38]. In fact, at low coverages the exact value of ϵ_1 hardly matters for the desorption spectra since almost no oxygen atoms are found at adjacent next-nearest neighbour sites.

For these small coverages of 0.03 ML and 0.19 ML, the simulated desorption spectra are peaked at about 775 K and 725 K (see Fig. 5) while the corresponding experimental peaks are found at slightly higher temperatures of

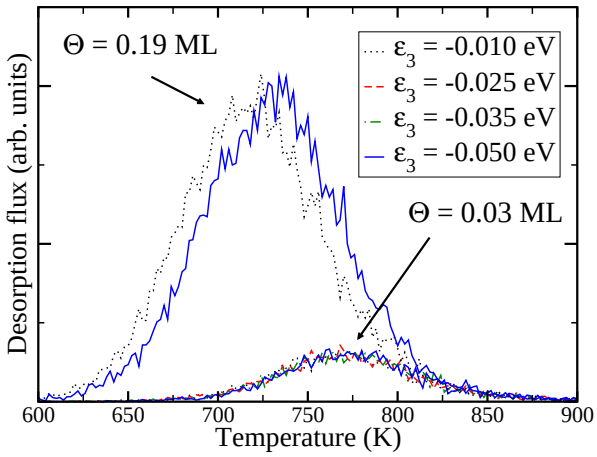

FIG. 5: Simulated TPD spectra of oxygen desorption for initial coverages of 0.03 ML and 0.19 ML and a heating rate of 4 K/s. The interaction parameter ϵ_3 was varied from -0.01 eV to -0.05 eV while $\epsilon_1 = 0.237$ eV and $\epsilon_2 = 0.04$ eV were kept constant.

814 K and 742 K [24], respectively. As Fig. 5 shows, for an initial coverage of 0.03 ML oxygen the spectra hardly change when ϵ_3 is varied from -0.01 eV to -0.05 eV. At these low coverage, only very few atoms find partners for the associative desorption. For higher attractive interactions, more atoms will be located within a distance of two lattice constants apart from each other because of the higher diffusion barrier for atoms that have a third next neighbour. At the same time, the desorption barrier is also higher. These two effects apparently cancel each other at a coverage of 0.03 ML.

At a coverage of 0.19 ML, the peak is significantly shifted to lower temperature which is indicative of the repulsive interaction between the oxygen atoms which effectively lowers the desorption barrier. Because of the higher coverage, which is close to the saturation coverage of oxygen when molecular oxygen is dosed to Pt(111), many oxygen atoms are located at third-nearest neighbor sites forming a $p(2 \times 2)$ structure. For this given structure, there is a dependence of the desorption flux on the interaction parameter ϵ_3. For a decrease of ϵ_3 from -0.01 eV to -0.05 eV, i.e. for a stronger attractive interaction between third-nearest neighbors, the desorption peak is shifted by 15 K to higher temperatures. If, on the other hand, the repulsive interaction between second-nearest neighbours (ϵ_2) is raised from 0.04 eV to 0.10 eV, the desorption peak is shifted by 15 K to lower temperatures (not shown in Fig. 5).

At high coverages, oxygen atoms also occupy next-nearest neighbor sites. These sites have the lowest desorption barrier; hence the value of ϵ_1 determines at which temperature the desorption starts. Using the value derived from DFT calculations, $\epsilon_1 = 0.237$ eV [38], the desorption spectrum exhibits a peak at 510 K for an initial coverage of 0.93 ML; in addition, the spectrum exhibits a second desorption peak (see Fig. 6). The first peak corre-

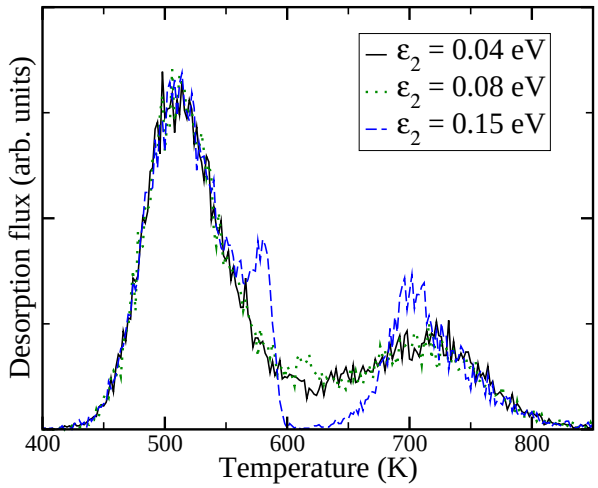

FIG. 6: Simulated TPD spectra of oxygen desorption for an initial coverages of 0.93 ML and a heating rate of 4 K/s. The interaction parameter ϵ_2 was varied from 0.04 eV to 0.15 eV while $\epsilon_1 = 0.237$ eV and $\epsilon_3 = -0.035$ eV were kept constant.

sponds to oxygen molecules desorbing associatively from oxygen atoms that are located at next-nearest neighbor sites. Due to the large value of ϵ_1, these sites become depleted before associative desorption from second- and third-nearest neighbors sites starts. Also a variation of ϵ_2 from 0.04 eV to 0.15 eV does not change this two-peak structure, as Fig. 6 shows.

Interestingly, the O_2 desorption spectrum after NO_2 exposures which leads to oxygen coverages up to 0.75 ML also shows a multiple peak structure [23] which is, however, not as pronounced as the one shown in Fig. 6. After O_3 exposure, on the other hand, the resulting TPD spectra are smoother [24], but still the desorption spectrum seemed to be composed from three different species. In the following, we will compare our results only with the experiments for ozone exposure.

For a coverage of 0.95 ML, desorption after ozone exposure at 300 K starts at about 500 K. In order to reproduce this desorption spectrum, we had to lower the value of ϵ_1. For lateral interaction energies of 0.10 eV, 0.04 eV and -0.035 eV for $\epsilon_{1,2,3}$, respectively, we obtained the TPD spectrum shown in Fig. 7 which agrees satisfactorily with the experiment [24]. With increasing coverage, the main desorption peak shifts to lower temperatures, indicative of the repulsive interaction between the adsorbed oxygen atoms. For the higher coverages, desorption takes place over the broad temperature interval between 500 K and 850 K. It should still be noted that while the position of the peak for a coverage of 0.93 ML at 625 K is rather close to the experimental one, the peak temperature for low coverages of about 775 K is too low compared to the experimental value of 814 K [24], as already mentioned. This is a hint that either the attractive interaction between third next neighbours (ϵ_3) is too small or that a larger value for the desorption barrier E_d^0 from the clean surface must be used.

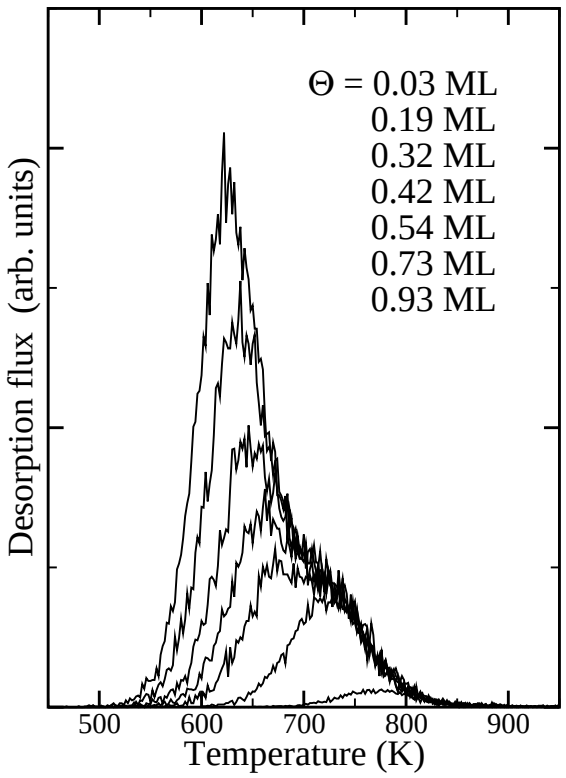

FIG. 7: Simulated TPD spectra of oxygen desorption for different initial oxygen coverages between 0.03 and 0.93 ML and a heating rate of 4 K/s. The interaction parameters were $\epsilon_1 = 0.10$ eV, $\epsilon_2 = 0.04$ eV and $\epsilon_3 = -0.035$ eV.

IV. DISCUSSION AND CONCLUDING REMARKS

Using the kinetic Monte Carlo algorithm, we have examined the dissociation, diffusion and desorption of oxygen interacting with Pt(111). The choice of the parameters entering the algorithm was motivated by previous experimental and theoretical studies, but they were adjusted in order to obtain agreement with the experiment. Using basically one set of parameters, we were able to reproduce results from different experiments such as STM studies or temperature programmed desorption for the wide temperature range from 100 to 900 K. Thus mechanisms proposed on the basis of experimental findings, for example for the oxygen chain formation at low temperatures [41], could be confirmed, and microscopic details of the elementary steps underlying the different processes could be revealed. Furthermore, the agreement between theory and different experiments lends credibility to the parameters used in the simulations. The parameters employed in the simulations in order to reproduce the experiments can thus be used as a benchmark in order to assess the accuracy of first principle results. For example, the used value of 0.36 eV for the molecular chemisorption energy lies in between the DFT values obtained with the popular functionals PW91 (0.6-0.8 eV [20, 27, 28]) and

RPBE (0.1 eV [28]), indicating that the PW91 functional overstimates the O_2-Pt(111) interaction while RPBE underestimates it.

It is still fair to say that it is not guaranteed that another set of parameters might not equally well reproduce all experimental findings. For example, the oxygen chains shown in Fig.4 have also been reproduced in another kMC study in a similar model, but with O_2 desorption and diffusion barriers that are much lower [42]. This kMC study was restricted, however, to the simulation of the growth of the oxygen chains and did not consider the associative desorption of oxygen. The reliability of the parameters might also suffer from the fact that the list of the considered microscopic processes could have been incomplete. However, the larger the number of different experiments that are reproduced within the same model, the more reliable the underlying parameters are. Thus we are rather confident that our simulations give a realistic description of the interaction of oxygen with Pt(111).

Acknowledgments

We thank Harald Brune for supplying us with data prior to publication.

[1] C. T. Campbell, G. Ertl, H. Kuipers, and J. Segner, Surf. Sci. **107**, 220 (1981).
[2] A. C. Luntz, M. D. Williams, and D. S. Bethune, J. Chem. Phys. **89**, 4381 (1988).
[3] C. T. Rettner and C. B. Mullins, J. Chem. Phys. **94**, 1626 (1991).
[4] A. E. Wiskerke, F. H. Geuzebroek, A. W. Kleyn, and B. E. Hayden, Surf. Sci. **272**, 256 (1992).
[5] B. C. Stipe, M. A. Rezaei, W. Ho, S. Gao, M. Persson, and B. I. Lundqvist, Phys. Rev. Lett. **78**, 4410 (1997).
[6] P. D. Nolan, B. R. Lutz, P. L. Tanaka, J. E. Davis, and C. B. Mullins, Phys. Rev. Lett. **81**, 3179 (1998).
[7] P. D. Nolan, B. R. Lutz, P. L. Tanaka, J. E. Davis, and C. B. Mullins, J. Chem. Phys. **111**, 3696 (1999).
[8] J. L. Gland, B. A. Sexton, and G. B. Fisher, Surf. Sci. **95**, 587 (1980).
[9] H. Steininger, S. Lehwald, and H. Ibach, Surf. Sci. **123**, 1 (1982).
[10] A. C. Luntz, J. Grimblot, and D. E. Fowler, Phys. Rev. B **39**, 12903 (1989).
[11] W. Wurth, J. Stöhr, P. Feulner, X. Pan, K. R. Bauchspiess, Y. Baba, E. Hudel, G. Rocker, and D. Menzel, Phys. Rev. Lett. **65**, 2426 (1990).
[12] C. Puglia, A. Nilsson, B. Hernnäs, O. Karis, P. Bennich, and N. Mårtensson, Surf. Sci. **342**, 119 (1995).
[13] A. N. Artsyukhovich, V. A. Ukraintsev, and I. Harrison, Surf. Sci. **347**, 303 (1996).
[14] J. Wintterlin, R. Schuster, and G. Ertl, Phys. Rev. Lett. **77**, 123 (1996).
[15] K. Gustafsson and S. Andersson, J. Chem. Phys. **120**, 7750 (2004).
[16] A. Groß, A. Eichler, J. Hafner, M. J. Mehl, and D. A. Papaconstantopoulos, Surf. Sci. **539**, L542 (2003).
[17] A. Groß, A. Eichler, J. Hafner, M. J. Mehl, and D. A. Papaconstantopoulos, J. Chem. Phys. **124**, 174713 (2006).
[18] A. Groß, in *The Chemical Physics of Solid Surfaces*, edited by D. P. Woodruff (Elsevier, Amsterdam, 2003), vol. 11, chap. 1.
[19] A. Eichler and J. Hafner, Phys. Rev. Lett. **79**, 4481 (1997).
[20] A. Eichler, F. Mittendorfer, and J. Hafner, Phys. Rev. B **62**, 4744 (2000).
[21] A. Groß, Surf. Sci. **500**, 347 (2002).
[22] N. Materer, U. Starke, A. Barbieri, R. Döll, K. Heinz, M. A. Van Hove, and G. A. Somorjai, Surf. Sci. **325**, 207 (1995).
[23] D. Parker, M. Bartram, and B. Koel, Surf. Sci. **217**, 489 (1989).
[24] N. Saliba, Y.-L. Tsai, C. Panja, and B. Koel, Surf. Sci. **419**, 79 (1999).
[25] B. Hammer, L. B. Hansen, and J. K. Nørskov, Phys. Rev. B **59**, 7413 (1999).
[26] J. P. Perdew, J. A. Chevary, S. H. Vosko, K. A. Jackson, M. R. Pederson, D. J. Singh, and C. Fiolhais, Phys. Rev. B **46**, 6671 (1992).
[27] M. Lischka, C. Mosch, and A. Groß, Electrochim. Acta **52**, 2219 (2007).
[28] P. Gambardella, Ž. Šljivančanin, B. Hammer, M. Blanc, K. Kuhnke, and K. Kern, Phys. Rev. Lett. **87**, 056103 (2001).
[29] A. Bogicevic, J. Strömquist, and B. I. Lundqvist, Phys. Rev. B **57**, R4289 (1998).
[30] D. S. Mainardi, S. R. Silva, A. P. J. Jansen, J. J. Lukien, and P. B. Balbuena, Chem. Phys. Lett. **382**, 553 (2003).
[31] K. A. Fichthorn and W. H. Weinberg, J. Chem. Phys. **95**, 1090 (1991).
[32] K. Reuter and M. Scheffler, Phys. Rev. B **73**, 045433 (2006).
[33] C. Sendner, S. Sakong, and A. Groß, Surf. Sci. **600**, 3258 (2006).
[34] A. P. J. Jansen, Phys. Rev. B **69**, 035414 (2004).
[35] P. Hänngi, P. Talkner, and M. Borkovec, Rev. Mod. Phys. **62**, 251 (1990).
[36] A. Groß, *Theoretical surface science – A microscopic perspective* (Springer, Berlin, 2002).
[37] H. Brune, J. Wintterlin, R. J. Behm, and G. Ertl, Phys. Rev. Lett. **68**, 624 (1992).
[38] H. Tang, A. van der Ven, and B. L. Trout, Phys. Rev. B **70**, 45420 (2004).
[39] P. Norton, J. Davies, and T. Jackman, Surf. Sci. **122**, L593 (1982).
[40] A. Winkler, X. Guo, H. Siddiqui, P. Hagans, and J. T. Yates, Jr., Surface Science **201**, 419 (1988).
[41] T. Zambelli, J. V. Barth, J. Wintterlin, and G. Ertl, Nature **390**, 495 (1997).
[42] A. Kersting and H. Brune, unpublished.